



Synchronization of Synchrotrons for bunch-to-bucket Transfers

T. Ferrand, H. Klingbeil / TEMF GSI-PBRF

H. Damerau / CERN BE-RF

Keywords: bunch-to-bucket, Synchrotron, Synchronization, Beam dynamic

Summary

To reach high particle energies with synchrotrons, a chain of several accelerators is required, as the ratio of extraction and injection energy is in the range of 10 to 20 per synchrotron. Hence the beam must be transferred from one accelerator to the next one. This document deals with the bunch-to-bucket transfer method to inject particle bunches composing the beam from a source synchrotron to a target synchrotron. After we highlight the theoretical concept of the bunch-to-bucket transfer, we determine physical limitations due to the beam dynamics and the adiabatic aspect of the particle bunches. A summary of the currently performed bunch-to-bucket transfer scenarios between the accelerators at CERN is given and set in relation with the mentioned theoretical concepts.



Contents

1	Introduction	3
2	General considerations on synchronization and phasing	3
2.1	Phase velocity of the buckets at transfer	3
2.1.1	Constraints due to energy matching	3
2.1.2	The synchronous particle	4
2.1.3	Condition on the buckets mean speed	4
2.2	Frequency setting and magnet field	5
2.2.1	The magnetic rigidity	5
2.2.2	Frequency setting according to geometrical specifications	5
3	Beam and particle position parameters	6
3.1	Beam parameters and physical limitations	6
3.1.1	Limitation on the frequency bump amplitude due to radial excursion	6
3.1.2	Synchrotron oscillations and adiabatic hypothesis	6
3.2	Matching in phase space	8
3.3	Phase advance	10
3.3.1	Phase-time equivalence	10
3.3.2	Correction of the phase advance	12
3.3.3	Fine correction phase locked loop	13
3.3.4	Control on the bunch spacing	13
4	Synchronous signals generation	13
5	Current implementation schemes at CERN	14
5.1	The accelerator chain at CERN	14
5.1.1	Proton protocol	14
5.1.2	Heavy ions	16
5.2	Synchronization and transfer specification	16
5.2.1	Transfer PS-Booster - PS	16
5.2.2	Transfer LEIR - PS	17
5.2.3	Transfer PS - SPS	18
5.2.4	Transfer SPS - LHC	19
6	Summary	21

1 Introduction

Accelerated particles accumulate energy every time they pass through the longitudinal electric field in the acceleration units. This energy is limited in a proton synchrotron by its capability of bending the beam trajectory. In order to attain higher energy levels, facilities benefiting from a larger magnetic rigidity have been designed. The combination of several criteria such as the technologies which are used to regulate the dynamic range of the magnet field and the specific space charge nonetheless allow only a restricted energy range of application for each accelerator. Thus the acceleration cycle needs to be split over several successive accelerators according to the expected beam energy and the features of each accelerator. A chain of accelerators consists typically of a Linac¹ and one or more synchrotrons designed to capture the beam at the extraction energy of the previous machine and to accelerate it to the injection energy of the next one.

Bunch-to-Bucket refers to the classical beam structure within a synchrotron. The beam is longitudinally kept together in so-called bunches in order to receive the correct energy from the electric field when passing through the RF² cavities. The relative positions in longitudinal phase space, where bunches can be held together are referred to as buckets. In the frame of a transfer sequence between two synchrotrons, the bunches are bumped towards their extreme trajectory and kicked out from their stable orbit in the source accelerator to be injected onto their stable orbit in the target accelerator. This transfer procedure requires the synchronization of the RF systems of both synchrotrons, so that the injected bunches reach the corresponding buckets in the target synchrotron. Bunch-to-bucket transfer refers thus to a very specific technical choice. Other possible implementations of extraction/injection processes will not be discussed in this document.

The document deals with the description of the synchronization and transfer of a train of bunches between two synchrotrons. In the general case, the target synchrotron already contains circulating bunches, which restricts significantly the control sequence degree of freedom. The synchronization sequence prior to the transfer can be split into three steps: the energy matching, the coarse synchronization and the fine synchronization. The energy matching sets the bunches revolution frequencies and the constraining magnet fields in order to have the bunches circulating with the same mean energy in both, the source and the target synchrotrons. The coarse synchronization shifts the bunch trains within the synchrotrons in order to temporally link a source bunch with a precise target bucket. The fine synchronization aims generally through a phase locked loop at correcting in real time the source bunches phase advance so that they hit exactly the center of the target buckets at injection. The voltage matching plays also its role at capture within the target synchrotron, avoiding quadrupole oscillations.

2 General considerations on synchronization and phasing

2.1 Phase velocity of the buckets at transfer

2.1.1 Constraints due to energy matching

The particle energy remains constant during a beam transfer. Therefore the source and the target synchrotrons must be matched regarding the energy of the circulating beams to pursue the acceleration [1]:

$$E_s = E_t. \quad (1)$$

The subscripts s and t refer respectively to the source synchrotron and to the target synchrotron.

¹Linac: Linear Accelerator

²RF: Radio Frequency

2.1.2 The synchronous particle

In order to relieve the mathematical representation of the bunch within the accelerator RF structure, calculations will often be performed on a single virtual particle, called synchronous particle. This synchronous particle is located at the fixed point of the particle trajectories in phase space. The general bunch behavior during RF manipulations can be approximated through computations of its synchronous particle.

The synchronous particle of charge q carries exactly the mean energy of its corresponding stationary bucket E_0 and sees exactly the desired accelerating electric field E_c at each passing through the cavity. Charged particles passing through an electric field are submitted to the Lorenz force, which is used in this case to transmit energy to the particle. The energy gain through the cavity of length l can thus be written as an integral:

$$\Delta E_0 = q \int_0^l E_c \cdot ds. \quad (2)$$

Assuming, that the applied RF voltage at the cavity gap is sinusoidal, the accelerating electric field may be written:

$$E_c = \frac{V_0 \sin \phi_0}{l}. \quad (3)$$

With V_0 , the RF voltage amplitude, ϕ_0 , the synchronous acceleration phase, i.e. the relative phase advance between the center of the bunch and the zero-crossing RF voltage and l , the length of the gap. This accelerating field is thus zero for the synchronous particle in a stationary bucket³. Replacing Eq.(3) in Eq.(2) and neglecting other external influences such as radiation losses⁴, we get the expression of the discrete energy variation per turn for the synchronous particle in a bunch of heavy ions in function of the applied RF voltage and the synchronous acceleration phase [2]:

$$\Delta E_0 = qV_0 \sin \phi_0. \quad (4)$$

2.1.3 Condition on the buckets mean speed

The speed of a stationary bucket and its revolution frequency are strictly equivalent for a given trajectory. The bunch velocity is defined as the relativistic fraction β of the speed of light c_0 . β can be defined for a particle using the mass ratio γ of its total energy E over its rest energy E_0 :

$$\gamma = \frac{E}{E_0}, \quad (5)$$

$$\beta = \sqrt{1 - \frac{1}{\gamma^2}}. \quad (6)$$

Since the synchronous particle must have the same energy at extraction and at injection:

$$\beta_s = \beta_t, \quad (7)$$

its speed remains constant during the transfer.

³Stationary bucket refers to a non-accelerated bucket (i.e. the synchronous phase $\phi_0 = 0$ or π)

⁴This assumption is not valid for leptons.

2.2 Frequency setting and magnet field

2.2.1 The magnetic rigidity

Magnetic fields are used to constrain accelerated particles on a closed trajectory. The more the particles' mean energy increases for a given trajectory, the stronger the field of the dipole magnets must be. The so called magnetic rigidity, namely the local product of the magnet field \mathbf{B} and of the bending radius ρ defines thus the maximum reachable energy for a particle type on the central orbit of the accelerator.

2.2.2 Frequency setting according to geometrical specifications

Synchrotrons have their path length L nearly constant at transfer energy. The synchronous particle's revolution frequency f_{rev} can be defined, neglecting slight variations from possible radial excursions (see beam parameters and physical limitations Sec. 3.1).

$$L_s \cdot f_{rev,s} = \beta \cdot c_0 = L_t \cdot f_{rev,t}. \quad (8)$$

From Eq.(8) we identify the nominal circumference ratio between two circular accelerators introducing N_s and N_t , two integer numbers resulting from the circumference ratio reduction:

$$\frac{f_{rev,s}}{f_{rev,t}} = \frac{L_t}{L_s} = \frac{N_s}{N_t}. \quad (9)$$

Eq.(9) explains the two-synchrotron-system periodicity in terms of synchronous particle revolution periods of each synchrotron. At transfer energy, assuming constant revolution frequencies, the whole system is exactly periodic every N_s synchronous particle revolution periods at $f_{rev,s}$ within the source synchrotron, which is also N_t synchronous particle revolution periods at $f_{rev,t}$ within the target synchrotron. The so called fiducial frequency f_c , which traduces this periodicity is therefore defined as the greatest common divider of the two revolution frequencies:

$$f_c = \frac{f_{rev,s}}{N_s} = \frac{f_{rev,t}}{N_t}. \quad (10)$$

A relation between the RF frequencies of both synchrotrons can be established by introducing the RF harmonic number h_{RF} into Eq.(9). In the following, we consider that the beam azimuth position and the phase of the RF signals are coupled by the beam phase loop.

$$f_{RF,s} = \frac{h_{RF,s} \cdot N_s}{h_{RF,t} \cdot N_t} f_{RF,t} \quad (11)$$

In their low energy regime most synchrotrons are equipped with ferrite or Finemet cavities. These cavities allow sweeps on a large bandwidth. The RF frequency and the mean magnetic field intensity in the synchrotron are linked by Eq.(14).

Assuming for a particle

$$p = q\mathbf{B}\rho = m_0\gamma\beta c_0 \quad (12)$$

and

$$v = \beta c_0 = c_0 \sqrt{\frac{\gamma^2 - 1}{\gamma^2}}, \quad (13)$$

one gets:

$$f_{RF} = \frac{h_{RF} c_0}{2\pi R_0} \frac{\mathbf{B}}{\sqrt{\mathbf{B}^2 + \left(\frac{E_0}{c_0 \rho q}\right)^2}} \quad (14)$$

with \mathbf{B} representing the bending field magnitude, E_0 , the synchronous particle rest energy and ρ the magnets bending radius. The velocity of light c_0 , the synchrotron mean trajectory radius R_0 and the synchronous particle charge q are constant.

Two main different philosophies are being considered at CERN and at GSI⁵, namely the direct RF frequency control according to a suitable magnet model, standard at GSI and the direct magnet field correction according to the main dipole magnets observation (called B-train, standard at CERN).

In the first case, the maximum ramping rate in the main dipole magnets defines maximum acceleration. The frequency ramp and the actual bending field amplitude are derived from the desired momentum profile (Eq.(12) and Eq.(14)). The control variable is the RF frequency. The bending field accuracy depends on the magnet models and on the quality of the control.

In the second case, the bending field is measured and corrected in real time (or evaluated through a model like at LHC) and used as a reference for generating RF frequencies. In the CERN synchrotrons, the magnet field control sequence results in a series of current pulses, which gives its name to this method. The RF frequency follows then the magnet field variations and regulation errors. In that case a finer frequency tuning prior to the transfer procedure must be performed in order to ensure its stability.

Independently from the implemented strategy, the RF frequency and the magnet field intensity for a given trajectory and energy are fully coupled.

3 Beam and particle position parameters

3.1 Beam parameters and physical limitations

3.1.1 Limitation on the frequency bump amplitude due to radial excursion

As previously highlighted, within a given synchrotron the magnetic field intensity \mathbf{B} , the radius of the beam orbit R , the momentum of its synchronous particle p and the revolution frequency f_{rev} are directly linked. Whereas the fundamental equation which links these parameters is non-linear [3], it can be easily locally linearized through four differential equations according to the relativistic mass factor γ . In particular, the relation which links the magnetic field intensity variations to the frequency and orbit radius variations is:

$$\frac{\Delta \mathbf{B}}{\mathbf{B}} = \gamma^2 \frac{\Delta f_{rev}}{f_{rev}} + (\gamma^2 - \gamma_{tr}^2) \frac{\Delta R}{R} \quad (15)$$

with γ_{tr} the value of γ at transition energy. For a constant magnetic field, the revolution frequency dependence from radial position offsets becomes:

$$\frac{\Delta f_{rev}}{f_{rev}} = \frac{\gamma_{tr}^2 - \gamma^2}{\gamma^2} \cdot \frac{\Delta R}{R} \quad (16)$$

Since radial feedbacks must be stopped during the transfer synchronization, the radial excursion must be kept within a very small range. Frequency modifications must take this parameter into concern. The range of the acceptable derivation depends on the synchrotron horizontal aperture but usually remains within a range of few centimeters or millimeters.

3.1.2 Synchrotron oscillations and adiabatic hypothesis

The synchronous particle describes the mean motion of the particles which are or could be circulating within the relative bucket. Whereas it represents a simplification of the general beam behavior and eases

⁵Helmholtzzentrum für Schwerionenforschung

its understanding, further beam physics limitations can not be considered under this assumption. To reach a deeper point of view in terms of bunch dynamics, the motion for non synchronous particles must be defined.

This may be done considering their motion with respect to the synchronous particle. By adapting Eq.(4) to the general case, defining ΔE as the difference between the synchronous particle energy E_0 from Eq.(4) and the non-synchronous particle energy E :

$$\Delta E = 2\pi\Delta R\dot{p} = qV_0(\sin\phi - \sin\phi_0). \quad (17)$$

Deriving Eq.(17) on the one hand and considering the so-called slippage factor η on the other, one can define the two fundamental equations Eq.(18) and Eq.(19) of the synchrotron oscillation [4].

$$\frac{d}{dt} \frac{\Delta E}{f_{rev}} \approx qV_0 \cdot (\sin\phi - \sin\phi_0) \quad (18)$$

$$\frac{d\phi}{dt} = \frac{h_{RF}\eta_0 f_{rev}}{p_0 R_0} \frac{\Delta E}{f_{rev}}. \quad (19)$$

Eq.(18) and (19) define an approximated Hamiltonian system [5], which results in the non-synchronous equation of motion:

$$\frac{d^2\phi}{dt^2} - \frac{h_{RF}\eta_0 f_{rev} qV_0}{p_0 R_0} \cdot (\sin\phi - \sin\phi_0) = 0. \quad (20)$$

Eq.(20) can be approximated for small amplitude synchrotron motions:

$$\frac{d^2\phi}{dt^2} + \Omega_0^2 \cdot (\phi - \phi_0) = 0, \quad (21)$$

with the so called synchrotron frequency

$$\Omega_0^2 = -\frac{h_{RF}\eta_0 f_{rev} qV_0 \cos\phi_0}{p_0 R_0} \quad (22)$$

and

$$\eta_0 \cos\phi_0 < 0. \quad (23)$$

Eq.(21) of the synchrotron motion can be solved as the linear pendulum problem equation. Generally for this problem type, the state variations are said adiabatic when they are slow enough compared with the system eigenfrequency. Introducing Eq.(22) in Eq.(20), the synchrotron equation can be written as follows:

$$\frac{d^2\phi}{dt^2} + \frac{\sin\phi - \sin\phi_0}{\cos\phi_0} = 0 \quad (24)$$

There are no strict analytical criteria for adiabatic beam manipulation but still an adiabatic transformation can be characterized according to Liouville's theorem as a transformation along which the Hamiltonian flux remains constant. Applied to the beam approximation, this condition is considered fulfilled when:

$$\alpha = \left| \frac{\frac{d\Omega_0}{dt}}{\Omega_0^2} \right| \ll 1, \quad (25)$$

assuming bucket trajectories close to the bucket center. α is called the adiabaticity parameter.

Integrating Eq.(20):

$$\left(\frac{d\phi}{dt} \right)^2 + 2 \left(\frac{h_{RF}\eta_0 f_{rev} qV_0}{p_0 R_0} \right) (\cos\phi - \cos\phi_0 + (\phi - \phi_0) \sin\phi_0) = C, \quad (26)$$

which approximates in second order:

$$\left(\frac{d\phi}{dt}\right)^2 + 2\left(\frac{h_{RF}\eta_0 f_{rev} q V_0}{p_0 R_0}\right) (\cos(\phi_0 + \Delta\phi) - \cos\phi_0 + \Delta\phi \sin\phi_0) = C, \quad (27)$$

$$\left(\frac{d\phi}{dt}\right)^2 + \left(\frac{h_{RF}\eta_0 f_{rev} q V_0}{p_0 R_0}\right) \cos\phi_0 \Delta\phi^2 = C. \quad (28)$$

Which is for a closed bucket trajectory of maximum phase excursion ϕ_m :

$$\frac{1}{\Omega_0^2} \cdot \left(\frac{d\phi}{dt}\right)^2 + (\phi - \phi_0)^2 = \phi_m^2. \quad (29)$$

Considering non-synchronous motions around a stationary bucket synchronous particle ($\phi_0 = 0$), Eq.(29) represents an ellipse in phase space centered on the bucket reference energy (E_0), whose axes ratio can be expressed as follows:

$$\left(\frac{\frac{d\phi}{dt}\Big|_m}{\phi_m}\right) = \Omega_0. \quad (30)$$

3.2 Matching in phase space

The amplitude of the particles' oscillations around the bucket synchronous particle is limited by the so-called separatrix. In Eq.(26), the term C depends on the particles' trajectory. The separatrix is defined for $\phi_{sep} = \pi - \phi_0$ and $\frac{d\phi_{sep}}{dt} = 0$ by

$$C_{sep} = \frac{h_{RF}\eta_0 f_{rev} q V_0}{p_0 R_0} [2 \cos\phi_0 - (\pi - 2\phi_0) \sin\phi_0] \quad (31)$$

All the trajectories in a bucket are centered around the stable phase ϕ_0 . The locations of the maximum momentum acceptance are determined by the stable phase independently from the trajectory constant. Introducing this consideration in Eq.(20), one obtains:

$$\frac{1}{2} \left(\frac{d\phi}{dt}\Big|_m\right)^2 = \frac{h_{RF}\eta_0 f_{rev} q V_0}{p_0 R_0} \cos\phi_0 \cdot (2 - (\pi - 2\phi_0) \tan\phi_0) \quad (32)$$

Introducing the over voltage factor $q = \sin^{-1}\phi_0$, the bucket height can be derived from Eq.(32) introducing Eq.(19):

$$\frac{\Delta E_m^2}{f_{rev}^2} = 2 \frac{q V_0 p_0 R_0}{h_{RF} |\eta_0| f_{rev}} \cos\phi_0 [2 - (\pi - 2\phi_0) \tan\phi_0]. \quad (33)$$

For a stationary bucket, Eq.(33) becomes:

$$\frac{\Delta E_m^2}{f_{rev}^2} = 4 \frac{q V_0 p_0 R_0}{h_{RF} |\eta_0| f_{rev}}. \quad (34)$$

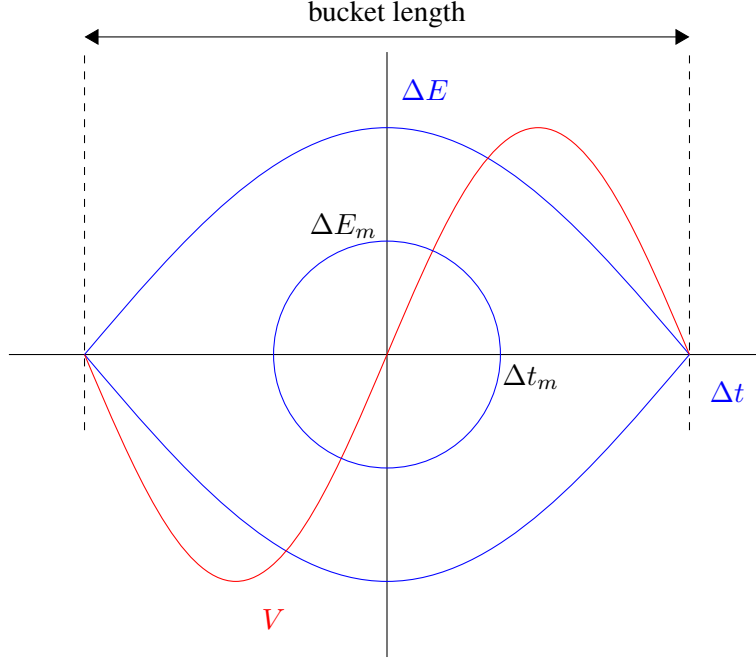


Figure 1: Phase-space representation of a bunch in its stationary bucket concurrently to its RF control function in red.

We consider that for a small phase variation around the bucket center, trajectories remain almost elliptic. Introducing the bucket elliptic longitudinal emittance ε as the maximum elliptic bucket area, which must remain a constant under adiabatic conditions:

$$\varepsilon = \pi \phi_m \Delta E_m, \quad (35)$$

From Eq.(19),

$$\Delta E_m = \frac{E_0 \beta^2}{4\pi^2 f_{RF}^2 |\eta|} \left. \frac{d\phi}{dt} \right|_m. \quad (36)$$

Using Eq.(30):

$$\Delta E_m = \frac{E_0 \beta^2}{4\pi^2 f_{RF}^2 |\eta|} \Omega_0 \phi_m. \quad (37)$$

$$\varepsilon = \pi \frac{E_0 \beta^2}{4\pi^2 f_{RF}^2 |\eta|} \cdot \sqrt{\frac{h_{RF} \eta_0 f_{rev} q V_0 \cos \phi_0}{p_0 R_0}} \phi_m^2. \quad (38)$$

With E_0 , β , p_0 and R_0 the energy, relativistic factor, momentum and trajectory radius of the corresponding synchronous particle. The maximum time length and energy spread of the considered elliptic trajectory expressed in function of the longitudinal emittance, introducing Ω_s in Eq.(38) correspond thus to the relations:

$$t_m^4 = \left(\frac{\phi_m}{2\pi f_{RF}} \right)^4, \quad (39)$$

$$= \frac{|\eta| h_{RF}}{2\pi^3 f_{RF}^2 E \beta^2 q V_0} \cdot \varepsilon^2 \quad (40)$$

and

$$\Delta E_m^4 = \frac{\varepsilon^4}{\pi^4 \phi_m^4}, \quad (41)$$

$$= \frac{2\pi f_{RF}^2 E_0 \beta^2 q V_0}{|\eta| h_{RF}} \cdot \varepsilon^2. \quad (42)$$

Perturbations of the longitudinal phase space distribution often result in quadrupole oscillations and in a longitudinal emittance blow up. To tackle this phenomenon, the receiving buckets should have the correct phase space trajectories to match the distribution of the injected bunches (see Fig. 1). To ensure that the receiving buckets have the correct energy acceptance regarding the transferred bunches, the RF voltage in both the sending and the receiving synchrotrons must be set accordingly [6][7].

Since we assume, that the beam in the transfer line does not suffer any energy loss, the synchrotron motion of the beam in both synchrotrons must have the same frequency. Eq.(22) leads for a stationary bucket, to

$$\frac{V_t}{V_s} = \frac{p_s R_s h_{RF,t} \eta_t f_{rev,t}}{p_t R_t h_{RF,s} \eta_s f_{rev,s}}. \quad (43)$$

At energy matching, introducing the circumference ratio Eq.(11)

$$\frac{V_t}{V_s} = \frac{R_s^2 h_{RF,t}^2 \eta_t}{R_t^2 h_{RF,s}^2 \eta_s} \quad (44)$$

3.3 Phase advance

3.3.1 Phase-time equivalence

Whereas bringing the beam of the source synchrotron to circulate at the same energy (i.e. at the correct velocity, according to the accelerator nominal ratio Eq.(9) and the respective harmonic number Eq.(11)) as the buckets in the target synchrotron is the first necessary requirement prior to the transfer, it does not represent the only condition. The bunches position at injection t_{inj} must coincide with their target bucket position as presented in the Fig (2) and Eq.(46).

$$t_{inj} = t_{ext} + \Delta t_{transfer}, \quad (45)$$

$$\Delta \phi_{bunch}(t_{inj}) \stackrel{!}{=} \Delta \phi_{bucket}(t_{inj}). \quad (46)$$

Since the target synchrotron may already contain a circulating beam, the choice of the target bucket is not a free parameter. Therefore it is important to locate (in terms of time) the bunches to be injected relatively to their expected target buckets. The phase advance of a bunch train within a circular accelerator can be evaluated with respect to an arbitrarily chosen azimuth at ϕ_{ref} :

$$\phi_{rev}(t) - \phi_{ref} = \left[2\pi \cdot \int_{t_{ref}}^{t_p} f_{rev}(t) dt \right]_{2\pi} \quad (47)$$

$$= [2\pi \cdot (t_p - t_{ref}) \cdot f_{rev}(t_{ref})]_{2\pi}. \quad (48)$$

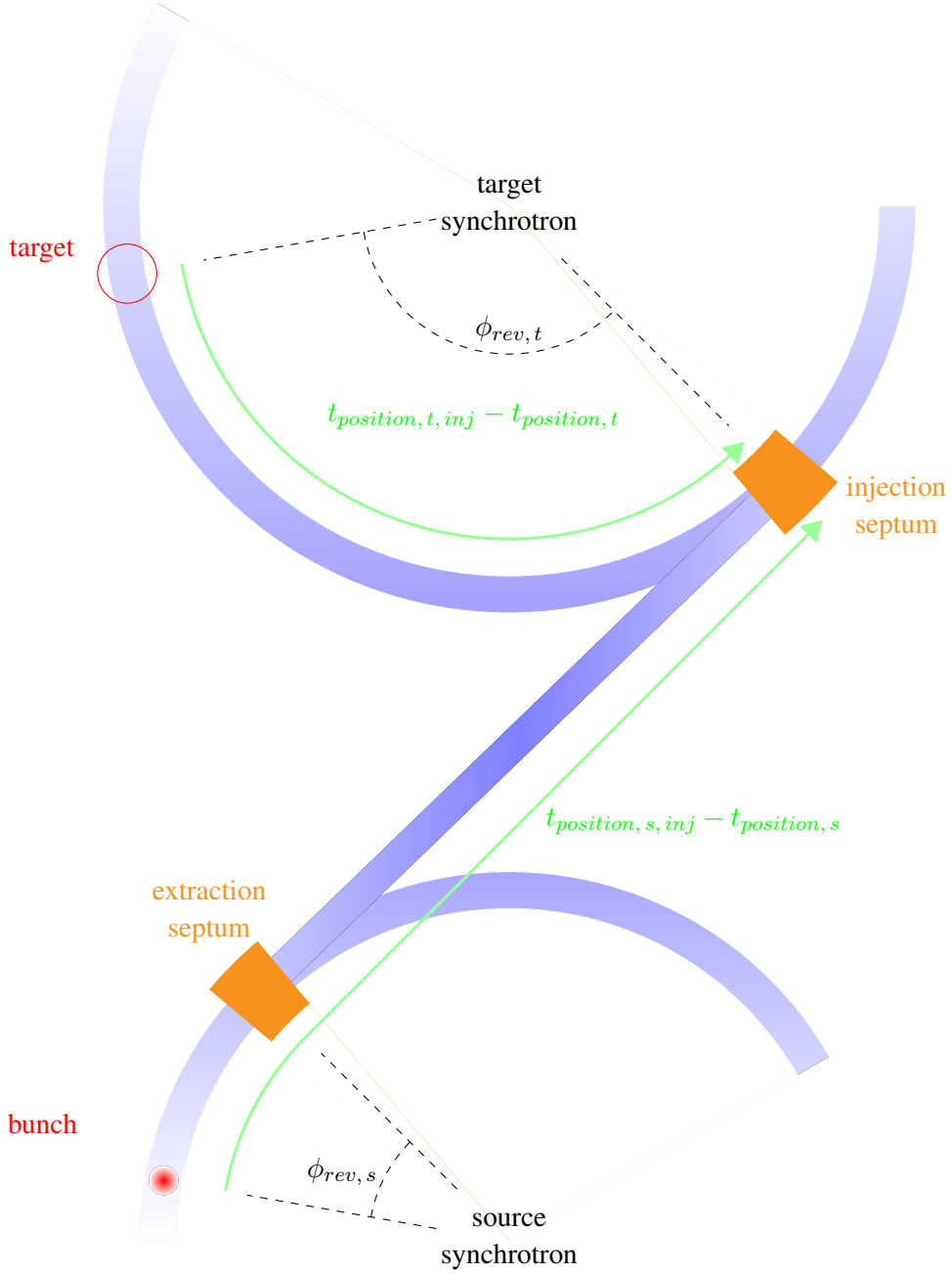


Figure 2: Time correspondence between an extracted bunch and its target bucket ($k = 0$).

As shown above, the whole stationary system of both accelerator is periodic with the frequency f_c , and at transfer energy both beams circulate with the same velocity. The transfer delay between the two synchrotrons is thus perfectly known. Applying the previous relation to both source and target synchrotrons, we evaluate each synchrotron target bucket position according to Eq.(49) and Eq.(50). The relative delay $\Delta t_{transfer}$ refers to the time needed by a bunch at the current velocity to travel through the transfer line from the ejection septum in the source synchrotron to the injection septum in the target synchrotron.

Considering the periodicity of each synchrotron, a phase advance can be written modulo a certain amount of revolutions. The relative phase advance between the positions of two bunches circulating in each synchrotron can thus be expressed as a periodical event, occurring every fiducial period, N_s turns for the

source synchrotron and N_t turns for the target synchrotron. If k is an amount of fiducial periods:

$$\Delta\phi_{bucket} = 2\pi \cdot k \cdot N_t + \phi_{rev,t} - \phi_{ref,t}, \quad (49)$$

$$\Delta\phi_{bunch} = 2\pi \cdot k \cdot N_s + \phi_{rev,s} - \phi_{ref,s}. \quad (50)$$

After identifying k , the condition (46) can be fulfilled at the injection point:

$$\Delta\phi_{bucket}(t_{inj}) = \Delta\phi_{bunch}(t_{inj}) \quad \text{in the target synchrotron,} \quad (51)$$

$$\Delta\phi_{bucket}(t_{inj}) = \Delta\phi_{bunch}(t_{ext}) + \Delta\phi_{transfer}, \quad (52)$$

$$k \cdot N_t + \phi_{rev,t}(t_{inj}) - \phi_{ref,t} = k \cdot N_s + \phi_{rev,s}(t_{ext}) - \phi_{ref,s} + f_{rev,s} \cdot \Delta t_{transfer}. \quad (53)$$

3.3.2 Correction of the phase advance

To fulfill Eq.(46), a frequency bump is introduced within the synchronization loop of one or both machines [8]. This frequency bump results in a phase slippage between the revolution resp. RF phase of each synchrotron as represented in the Fig (3). Δt_{ref} represents the possible delay between the two reference azimuths within the source and target synchrotrons. These two reference azimuths must not necessarily be set at the same time as long as they are linked through a unique relation. Considering a revolution frequency variation $\Delta f_{rev}(t)$ during the bump, the shift in terms of time can be calculated using the frequency mean value over the phasing \hat{f}_{rev} :

$$\Delta t_{phasing} = \frac{\Delta\phi_{phasing}}{2\pi \cdot \hat{f}_{rev}} \quad (54)$$

$$= \frac{\int_{t_0}^t \Delta f_{rev}(t) dt}{\hat{f}_{rev}} \quad (55)$$

The resulting time $\Delta t_{phasing}$ must then coincide with the time position difference due to the transfer line, which is introduced through the transfer and with the respective reference times of each synchrotron.

This so-called cogging operation represents the actual targeting of a reference bucket in the target synchrotron. The bunch train is temporally shifted with respect to the circulating beam in the target synchrotron.

The technological means that are used to perform this bunch train re-phasing generally allow positive as well as negative frequency bumps. In most cases the target synchrotron is considered as providing the frequency reference signals during the synchronization procedure and the frequency bump is thus only applied to the source synchrotron, whereas both synchrotron RF and revolution signals can theoretically be shifted since only the relative shift is taken into account. The same procedure is used e.g. in the LHC to move the collision point in the center of the experiments.

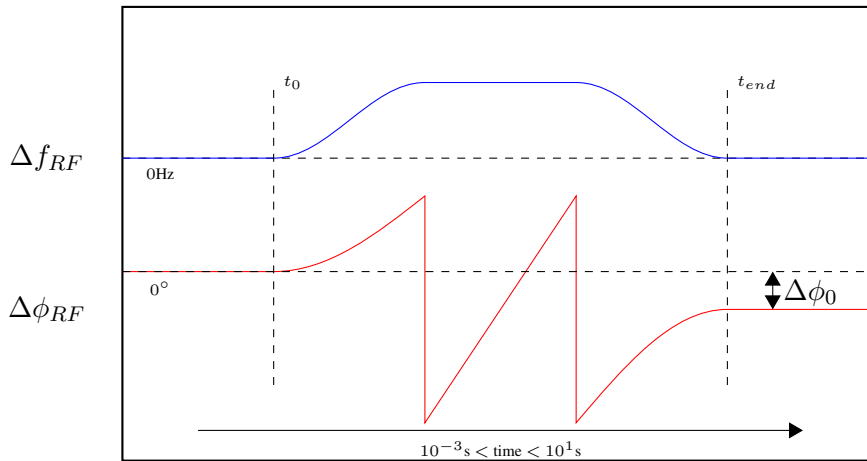


Figure 3: Relative phase beating and frequency slippage between two RF signals. The frequency slippage between the RF frequencies of two synchrotrons is represented in blue. The resulting phase beating is represented in red.

3.3.3 Fine correction phase locked loop

Considering the relation between RF and revolution frequencies, it appears that any phase errors at the revolution frequency has a h_{RF} times higher impact on the RF phase, and thus on the actual bunch to bucket phase offset. To improve precision, a second phase correction is then needed after the revolution phase correction to align the bunches to the bucket centers. Generally a phase locked loop is locked on a shared frequency $f_{inj} = h_{RF} \cdot f_{rev, inj}$, corresponding to the desired energy level to ensure a reliable control on the RF phase of each bucket and to limit the filamentation at injection. The reference frequency can be generated externally and thus must not necessarily be exactly equal to existing RF or revolution frequencies.

In some cases like at LEIR⁶, specific correction functions have been implemented to improve the behavior of the control loop.

3.3.4 Control on the bunch spacing

In the case of a stationary bucket, the RF control signal, which forms a bucket in longitudinal phase-space sets its height and time length as illustrated in the Fig.1.

The bucket area can be evaluated according to Eq.(56) as a function of the synchronous particle charge q , the synchronous particle relativistic ratio β , the synchronous particle total energy E_s , the so called slippage factor $\eta = 1/\gamma_{tr}^2 - 1/\gamma^2$ and a non linear function depending on the synchronous particle revolution phase $\alpha(\phi_s)$ in a more general case but whose value is 1 for a stationary bucket.

$$A = \frac{8\sqrt{2}}{2\pi f_{RF}} \sqrt{\frac{E_0 \beta^2 q V_0}{\pi h_{RF} |\eta|}}. \quad (56)$$

The time length of a stationary bucket is:

$$\Delta t_{bucket} = \frac{1}{f_{RF}} = \frac{1}{h_{RF} \cdot f_{rev}}, \quad (57)$$

and thus that the maximum amount of buckets on the beam orbit is exactly h_{RF} . However, not all of these buckets are necessarily filled and empty gaps may be left to allow the setting of the kickers field at beam transfer.

4 Synchronous signals generation

This section deals with the signal sharing point of view within a system of two or more synchrotrons. As a general assumption, the device responsible for the actual generation of these synchronous signals will be considered as a third device which could actually, according to each case, be integrated into the RF system of whether the source synchrotron or the target synchrotron or any other existing system. What will be depicted here as signal generation system must be seen as a function more than as a real device.

This signal generation system has two main roles:

⁶LEIR: Low Energy Ion Ring

1. Its first role is to provide to all the actors of the synchronization/transfer process a stable and reliable time, respectively frequency reference. One of the main tasks of the source synchrotron is to align its bunches on empty buckets within the target synchrotron, that is the two RF systems must be able to communicate but this communication covers also some uncontrollable delays. The signal generation system must thus ensure that the synchrotron which receives an information is able to link it with a precise time stamp and resynchronize it according to a shared clock reference. In most cases the same time reference is considered for both source and target synchrotrons $\Delta t_{ref} = 0$. This ensures also that the bucket counting refers to the same moment in both accelerators.

To fulfill this first role, several possibilities exist like at CERN where the fiducial frequency is often derived from the target synchrotron revolution signal and sent to the source synchrotron. This feature allows a slightly variable fiducial frequency as it is, for instance, generated for the second PSB⁷-PS⁸ transfer. In this case $f_c = f_{rev, PS}$ is derived from the PS closed-loop RF and hence, represents a moving target. The PSB synchronizes on this slightly variable fiducial frequency signal. For larger facilities like PS and SPS⁹, only the first bunch must be synchronized with its target bucket since the bunch spacing is a multiple of the RF period by definition. At GSI, both synchrotrons are expected to be synchronized on an external $f_c \approx f_{rev, SIS100}$ signal, which would be derived directly from the BuTiS¹⁰.

2. Its second role before the transfer itself is to ensure the synchronization between the extraction from the source synchrotron and the injection in the target synchrotron, which means, to procure the reference signals with respect to which the extraction and injection kickers must be triggered to ensure the capture of the transferred beam. It must take into account the rising time of magnet fields of both synchrotrons, the bunch spacing in each accelerator and the transferred beam time of flight.

To fulfill the second role and thus ensure, that all the elements of the transfer chain are actually synchronized taking their relative delays into account, the fiducial frequency signal is shifted in both synchrotrons in order to introduce a known time offset between their RF systems. After the resynchronization, both synchrotrons are expected to refer to the same signal exactly at the same time with a certain jitter, which should be negligible compared with the actual period of the signal.

At GSI, this reference signal is expected to be derived from the shared clock, which has a low picosecond jitter using DDS¹¹ modules. The transmission time offset could then be compensated during the signal generation or at the signal reception.

5 Current implementation schemes at CERN

5.1 The accelerator chain at CERN

5.1.1 Proton protocol

The LHC¹² injection chain at CERN is optimized for protons. From a source, protons are injected into a linear accelerator, currently LINAC-2. Protons are accelerated to an energy of 50 MeV (kinetic) [9].

⁷PSB: PS-Booster

⁸PS: Proton Synchrotron

⁹SPS: Super Proton Synchrotron

¹⁰Bunchphase Timing System

¹¹Direct Digital Synthesizer

¹²Large Hadron Collider

	PSB	->	PS	->	SPS	->	LHC	[units]
circ.	157.1		628.3		6911.5		26659	[m]
$\frac{N_e}{N_s}$ ratio		4		11		7/2		
filling	1		2 PSB		2/3/4 PS		12 SPS	cycles
pattern	1		4+2->72		144/216/288			
Tr. Energy		1.4		26.0		450		[GeV/u]
h_{RF}	1+2		7->21->84		4620			
Tr. ϵ		1		0.35		0.60		[eVs]
f_{rev}	0.6->0.7		3.1/9.3->10/40		200.4		400.8	[MHz]
spacing			327->25					[ns]
fiducial sig- nal		$//f_{rev, PS}$		$//f_{rev, SPS}$		$//\frac{f_{rev, LHC}}{7}$		
inj. signal				$//f_{RF, PS}$		$//f_{RF, LHC}$		
course sync.	$h_{PSB,1}$ or $h_{PSB,2}$		$h_{PS,1}$		$h_{SPS,1}$			
fine sync.	<i>none</i>		$h_{PS,84}$					

Table 1: Transfer parameters

Pre-accelerated proton bunches are then injected into the first synchrotron of the chain, namely PSB. The PSB is composed of four identical rings of 157.1 m circumference stacked on the top of one another. This acceleration stage carries the proton bunches up to 1.4 GeV ($\beta = 0.916$). To produce an LHC-beam, PSB accelerates nominally one bunch per ring at $1.6 \cdot 10^{12}$ protons/bunch.

The protons with an energy of 1.4 GeV are injected into the PS. The PS is a combined function alternating gradient synchrotron. With its circumference of 628.3 m, the PS is exactly 4 times larger than a single PSB ring. It is composed of one ring equipped with 100 bending magnets. Injection in the PS for normal LHC-type beams is composed of a first injection of one bunch per PSB ring and a second injection of only two PSB bunches, that corresponds to a filling ratio in the PS of 6/7 ($h_{RF} = 7$), leaving a gap for the extraction kickers. The role of the PS in the LHC injection scheme is to prepare the bunch structure for the LHC ($1.3 \cdot 10^{11}$ p/bunch intensity, 4 ns long bunches spaced by 25 ns for an energy of 26 GeV, $\beta = 0.999$).

Proton beams must be accelerated further to reach the LHC injection energy of 450 GeV and additional blow-up must be applied to reach the longitudinal emittance of 0.6 eVs. The SPS is a separated function alternating gradient synchrotron of 6911.5 m circumference, 11 times larger than the PS, equipped with a traveling wave RF system at 200 MHz with a higher harmonic system at 800 MHz, that enables special acceleration and RF manipulation features. Bunches for LHC beams are prepared in the PS so that no further RF manipulation is needed in the SPS. One SPS cycle results in 2, 3 or 4 PS cycles for the respective total beam intensity in the SPS of 1.7, 2.5 or $3.3 \cdot 10^{13}$ p/beam.

The proton bunches are finally injected in the LHC. The LHC is a superconducting dipole technology based collider composed of two rings, each of 26.659 km circumference and equipped with 8 accelerating cavities, which generate a 400.8 MHz RF structure. The SPS bunches blow up by about 25% at injection because of an intrinsic voltage mismatch. The filling of each LHC injection requires 12 SPS cycles. The acceleration until 7 TeV lasts 20 minutes due to the magnet current ramp limitation, which leads to a maximum energy gain of 485 keV/turn. At the end of an LHC cycle the beam is composed of up to 2808 bunches at $h_{RF} = 3564$ with a longitudinal emittance of 2.5 eVs each.

At CERN, the target synchrotron provides the frequency reference. The source synchrotron synchronizes on this reference disregarding the filling state of the target synchrotron. A phase offset in the reference signals enables to select the desired bucket for injection.

5.1.2 Heavy ions

Heavy ions like lead and argon ions are produced at CERN by an ECR¹³ ion source and sent to LINAC-3 to reach the energy of 4.2 MeV/u required for injection into the LEIR. The LEIR injects its beam in the PS at the equivalent energy of 72 MeV/u. The later acceleration and transfer cycles are sensibly the same as for proton beams except for some specific fixed frequency manipulations in the SPS. Lead ions reach after a complete cycle 2.76 TeV/u.

5.2 Synchronization and transfer specification

5.2.1 Transfer PS-Booster - PS

The most specific feature, which can be found at CERN is certainly the use of a B-train in most of its accelerators. The use of the B-train results in the fact, that a magnet measurement system transmits the dipole field through a series of **B**-field corrections. The magnet, which is used for this measurement is a complete dipole magnet electrically in series and identical to those actually used to guide the beam path,

¹³ECR: Electron Cyclotron Resonance

but placed outside the accelerator tunnel, where its magnet field can easily be measured. In some recent accelerators at CERN, e.g. AD¹⁴ or LHC, this B-train is simulated according to a stored magnetic cycle but the main principle remains exactly the same.

Theoretically the RF frequency which is applied at the cavities can be derived from the direct measurement of the magnet field over the B-train according to the Eq.(12) but all the parameters (**B**-field, orbit radius, etc.) are not necessarily known during the synchronization procedure, due to tune shift and quadrupole oscillation.

A procedure between PSB and PS has been developed in order to correct these uncertainties. First, both accelerators are set at the expected RF frequency depending on the desired transfer energy level. The choice of the transfer RF frequency depends on some additional constraints, as the PS has fixed frequency VHF¹⁵ (200 MHz) cavities. To operate them on the flat bottom without exceeding their frequency range, the revolution frequency in the PS must be fixed to an integer, sub-multiple of their resonance frequency ($f_{RF,200MHz} = 458 \times f_{rev} = 436.568$ kHz). A frequency bump is used to align the test-bunch of the PSB on a desired PS bucket seen as a moving targets [10].

When the energies relative to the bunch trajectories within both synchrotrons do not perfectly match, a longitudinal emittance blow-up and an important radial offset can be observed. Measuring the debunching at injection at the PS without RF control, the new matching requirements can be computed [11]. The field produced by the PS dipole magnets is then corrected according to these measurements:

$$B_{new}^{PS} = B_{old}^{PS} \cdot \left(1 - \gamma^2 \cdot \frac{\Delta f}{f_{rev}^{PS}} - (\gamma^2 - {}^{PS} \gamma_t^2) \cdot \frac{\Delta R}{R^{PS}} \right). \quad (58)$$

This method results in a slight change in the transfer energy level, therefore the magnet field (and thus the RF frequency) in the Booster must be adjusted according to:

$$B_{new}^{Booster} = B_{old}^{Booster} \cdot \left(1 - (\gamma^2 - {}^{PSB} \gamma_t^2) \cdot \left(\frac{\Delta f}{f_{rev}^{PS}} + \frac{\Delta R}{R^{PS}} \right) \right). \quad (59)$$

This procedure normally takes place about once a year between the two accelerators and for each of the four quasi-independent rings in the specific case of the transfer PSB-PS.

As mentioned the PS filling procedure from the PSB is composed of 2 PSB cycles. During the first one, the target bucket at PS can be chosen arbitrarily since no bunch circulates in its ring. Only the four PSB extractions must be de-phased from one another by exactly the expected bunch spacing defined by the PS RF structure.

After the PS sends the transfer requirement for the first injection, a warning pulse indicating 10 ms before transfer is generated synchronously with the fiducial pulse signal (and delayed by half a revolution period to avoid the ‘‘chevauchement des flancs’’). The two synchrotrons revolution frequency signals are then delayed with respect to the fiducial frequency signal and with the actual revolution signal of the PS (which is here the target synchrotron). A pulse is generated at 2 ms before transfer synchronously with both synchrotron revolution signals. The time of flight between the two synchrotrons and the triggers for measurement instrumentation are then generated by counting the PS and PSB revolution periods. For the second transfer, the synchronization is performed in closed loop with distributed signals in the PS.

5.2.2 Transfer LEIR - PS

The LEIR being equipped with a fully digital RF beam control and Finemet cavities, the synchronization approach between the LEIR and the PS is the same as for protons between the PSB and the PS. However, since ions need no blow-up on the PS flat-bottom, the RF frequency at injection can be set to a arbitrary value within the range of frequencies of both accelerators.

¹⁴AD: Antiproton Decelerator

¹⁵VHF: Very High Frequency

5.2.3 Transfer PS - SPS

As developed earlier, once the two synchrotrons are set to the same energy prior to the transfer, the bunch train must be re-phased to face the desired train of buckets in the target synchrotron. Assuming that the bunch-spacing in both accelerators coincides, that is the bunch-spacing in the PS must be consistent with the distance of bucket centers in the SPS (for a LHC-beam, $f_{RF,PS} = 40$ MHz, $f_{RF,SPS} = 200$ MHz), the relative time delay (or the equivalent phase) between the first bunch of the train to be sent and the reference bucket of the receiving train can be evaluated.

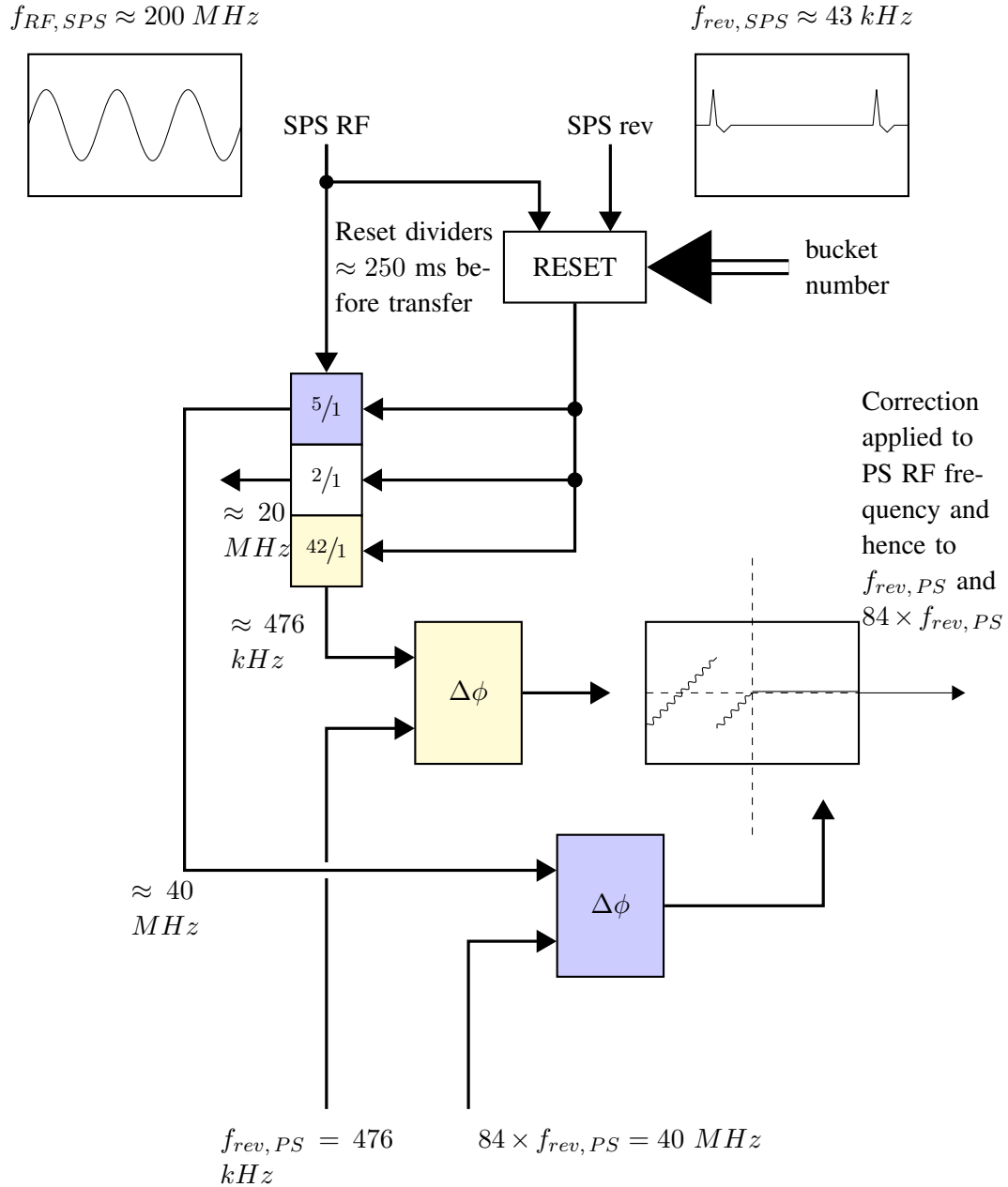


Figure 4: PS-SPS synchronous signals generation procedure. The actual coarse synchronization chain is colored in light yellow. In blue is the phase locked loop discriminator for fine synchronization represented.

Considering the integer circumference ratio between the PS and the SPS of:

$$C^{SPS} = 11 \cdot C^{PS} \quad (60)$$

the fiducial frequency can be assimilated to the SPS revolution frequency according to Eq.(9). The RF frequencies are set at the same value, therefore the injection frequency can be directly derived from the SPS RF system.

1. The SPS shares a pulse train at frequency f_c and a sine-wave at f_{inj} through optical fibers. These two signals are generated concurrently to its actual signals at $f_{rev,SPS}$ and $f_{RF,SPS}$ but are not corrected by any feedback loop.
2. A series of frequency dividers is used to generate a signal around

$$\begin{aligned} &\approx f_{rev,PS} = 476 \text{ kHz needed for the coarse synchronization,} \\ &\approx 42 \times f_{rev,PS} = 20 \text{ MHz needed for instrumentation and,} \\ &\approx 84 \times f_{rev,PS} = 40 \text{ MHz needed for the fine synchronization} \end{aligned}$$

from the injection signal (see Fig.(4)).

3. The fiducial frequency signal is used as a reference for the bucket numbering. A reset mechanism, which is kept synchronous with the injection signal ensures a correct bucket centering.
4. The phase evaluation during the coarse synchronization is performed on the PS revolution frequency and the 476 kHz SPS-derived signal by a phase discriminator. The frequency bump duration depends on this phase measurement.
5. Once the bunch train is shifted at the correct time position on its trajectory to fit to the train of target buckets, the fine synchronization loop locks on the 40 MHz SPS-derived signal. A $84 \times f_{ref,PS}$ signal using this second phase discriminator holds the phase advance between the reference bunch within the source synchrotron and the reference bucket within the target synchrotron constant until the transfer. This assures the correct alignment of the bunches with respect to the target bucket centers.

After the transfer requirement has been sent, a warning pulse is generated from the SPS 10 ms before transfer. A delay is introduced between the PS RF signal and its relative fiducial, revolution and RF pulse signals in order to avoid “chevauchement des flancs”. The SPS revolution and RF pulse signals are also delayed from the actual SPS RF signal. Warning pulses synchronous with the revolution frequency signals of both synchrotrons are then generated 8 ms and then 2 ms before transfer. The delays relative to the time of flight and the instrumentation are then ensured by counting the PS and SPS revolution periods like between PSB and PS.

5.2.4 Transfer SPS - LHC

LHC is a very particular case at CERN because of its large dimensions, which result in a significantly longer maximum bunch train synchronization time, because the nominal ratio between SPS and LHC is non-integer and because the B-train is completely simulated from a stored magnetic cycle. The fiducial relation being:

$$f_c = \frac{f_{rev,LHC}}{7} = \frac{f_{rev,SPS}}{27} = 11.245 \text{ kHz}, \quad (61)$$

and setting the harmonic number to:

$$h_{RF,LHC} = 2 \frac{27}{7} h_{RF,SPS}, \quad (62)$$

the RF frequency which is used as injection frequency responds to:

$$f_{inj} = \frac{f_{HF,LHC}}{2} = f_{HF,SPS}. \quad (63)$$

During the synchronization procedure the SPS plays the same role than the PSB in the transfer PSB-PS or than the PS in the transfer PS-SPS and follows the reference signals coming from the LHC through optical fibers. The LHC signal generation system delays its fiducial signal with respect to its revolution signal to force the SPS to target the right bucket like represented on the Fig.(6).

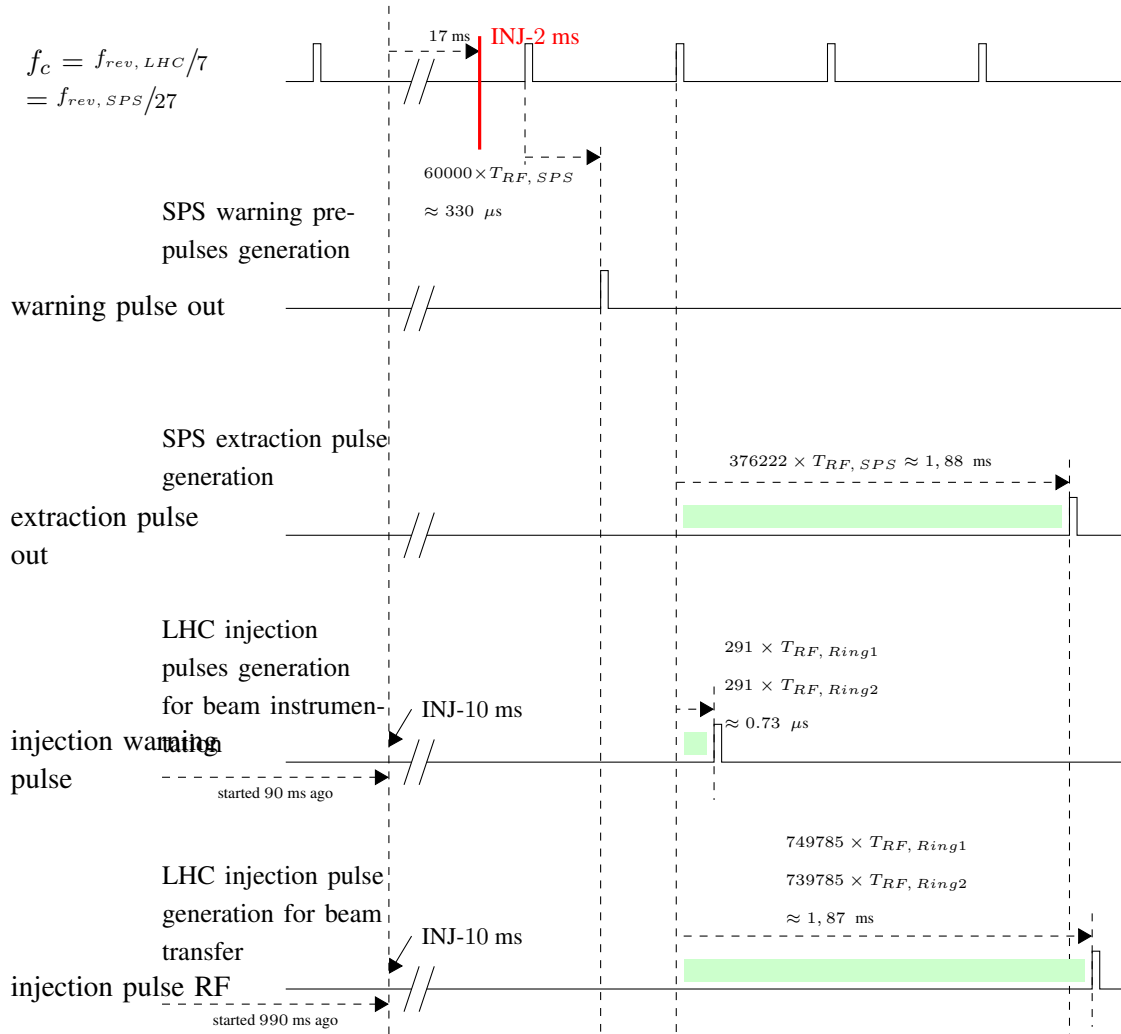


Figure 5: Synchronous signal generation time schedule at pre-transfer for a typical SPS-LHC transfer

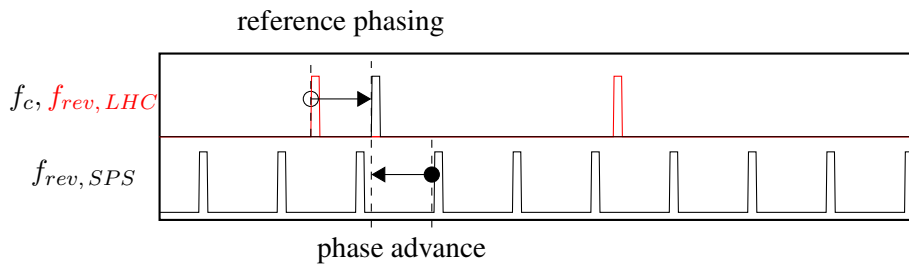


Figure 6: Batch synchronization for SPS-LHC transfer: revolution signals sliding

The theoretically simplest bump function, which responds to the constraints on the maximum frequency variation and on the adiabatic hypothesis can be written as follows:

$$f(t) = a \cdot t - \frac{2^4}{3^3} \frac{a^3}{\Delta f^2} t^3, \quad (64)$$

with a , the maximum frequency change rate during the bump. The bump duration would then be:

$$\Delta t = \frac{3 \Delta f}{2 a}. \quad (65)$$

In the frame of the SPS-LHC transfer a more sophisticated bump function is currently used in the SPS:

$$f(t) = \frac{\Delta f}{2} + a \cdot \left(t - \frac{3 \Delta f}{4 f} \right) - \frac{2^4 a^3}{3^3 \Delta f^2} \left(t - \frac{3 \Delta f}{4 a} \right)^3 \quad (66)$$

With $a = 7$ Hz/s. The fine synchronization is also completely handled by the LHC, which delays the injection signal with respect of its RF signal, on which the SPS triggers its own RF signal as shown on the Fig.(7). In both cases the hardware delays are compensated, synchronizing the shared signals using additional controlled delays.

Considering the worst case, SPS must shift its beam by 180° to target the expected buckets in the LHC. The complete procedure is likely to last up to 12 s for heavy ions but according to the nominal ratio between SPS and LHC, one turn LHC corresponds to $4 - 1/7$ turns SPS. That is, preferring the LHC periods to the fiducial periods for performing the bunch train shifting enables to minimize the re-phasing to at most $360/14^\circ$ which corresponds to less than 2 s providing the re-phasing can be performed both with a negative or a positive frequency bump.

Like in the previous cases, a phase locked loop set on a delayed image of the injection frequency (two times the SPS RF frequency) is used to ensure the fine synchronization (see Fig.(7)).

Fig.(5), sums up the steps of the synchronization of the LHC and SPS RF systems. After a pre-implemented delay, the signal generation system triggers a counter system on a fiducial pulse signal and then counts a certain amount of SPS revolution periods, corresponding to half the fiducial period to get the maximum jitter margin and thus cancel the uncertainty on the trigger slope due to “chevauchement des flancs”.

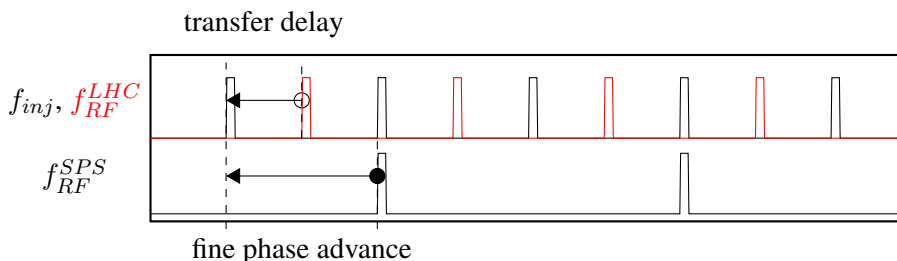


Figure 7: Fine phasing at SPS-LHC: RF signals sliding

6 Summary

This document highlights only a few points, which compose the Bunch-To-Bucket transfer problem. We observe that the synchronization procedure can be performed without taking unpredictable effects like natural beam oscillations and tune shift into consideration, which is relevant only under some special conditions.

The remarkable fact is, that whereas the Bunch-To-Bucket transfer is currently performed according to very similar procedures in the different existing accelerator chains over the world, they are highly dependent on implemented technologies and timing philosophies.

The Bunch-To-Bucket transfer is therefore a specific procedure, which is computed especially for each source/target/ion type combination. We aim at increasing the efficiency and the flexibility of this beam transfer for further implementations.

This document is expected to be updated in the future. Figure 8 proposes an overview on the two main possible acceleration chains at CERN for protons and lead heavy ions.

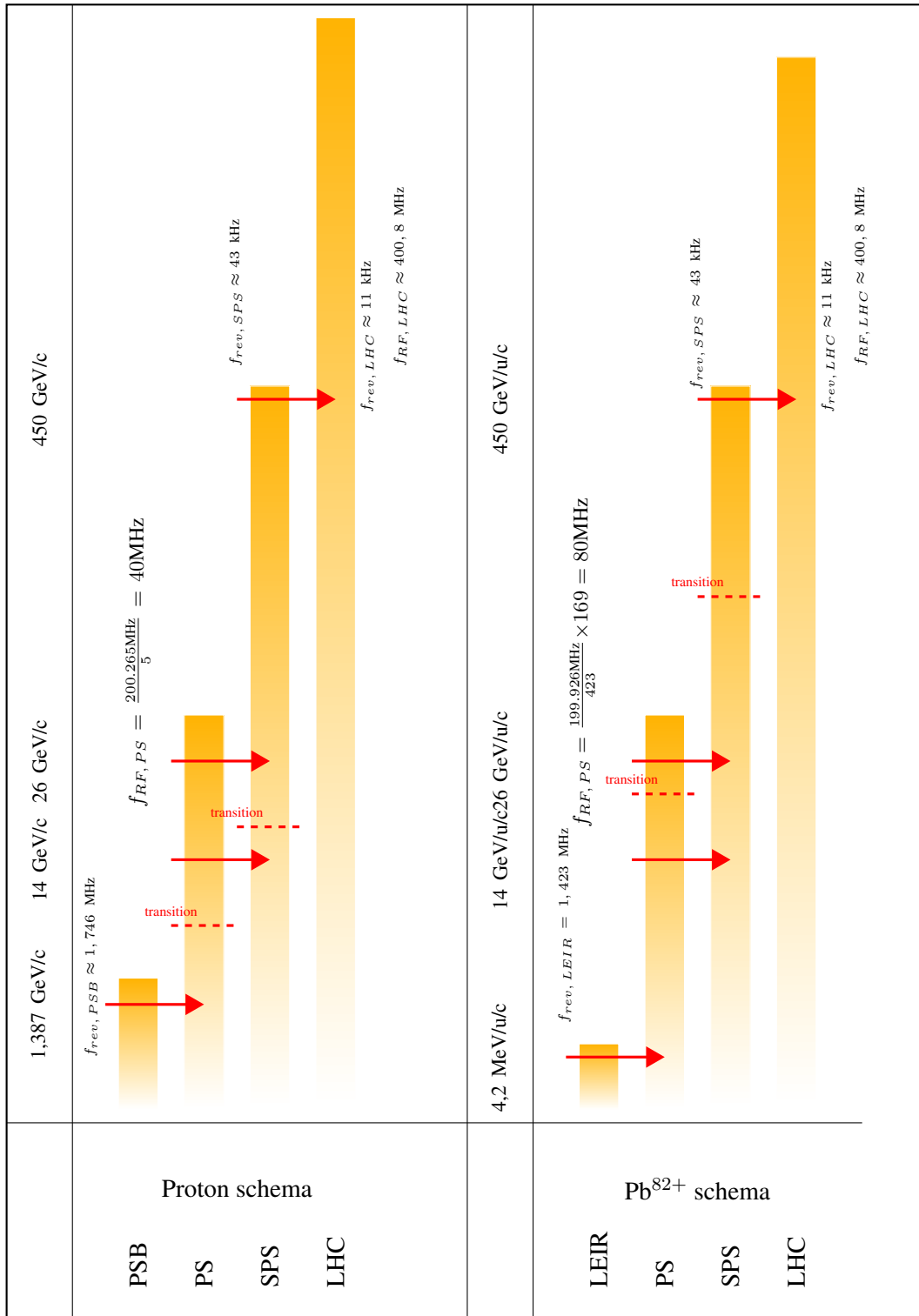


Figure 8: Energy matching overview at CERN between PSB, LEIR, PS, SPS and LHC. . The orange shaded lines represent qualitatively the operational frequency range. The frequency working ranges are represented unscaled.

Acknowledgments

This document has been produced after my two first visits at CERN (17/02/14 - 17/03/14 and 16/03/15-27/03/15) which couldn't have happened without the implication of Heiko Damerau and Harald Klingbeil, to who I am very grateful. I want to thank especially Maria Elena Angoletta, Philippe Baudrenghien, Thomas Bohl and Elena Chapochnikova for their patience, their help and their worthy advises. I thank also all the staff of the BERF on the Preveessin site for the great work atmosphere and their support.

References

- [1] R.J. Laucher. "Matching the Energy of CPS and SPS Machines". In: CERN-SPS-AMS-Note-88-1 (1988).
- [2] S. Henderson and A. Aleksandrov. *Beam Dynamics in Proton Linacs*. Third. ISBN-10 981-02-3858-4, ISBN-13 978-981-02-3858-4. Alexander Wu Chao and Maury Tigner, 2009, p. 365.
- [3] C. Bovet; R. Gouiran; I. Gumowski; K.H. Reich. *A Selection of Formulae and Data Useful for Design of A.G. Synchrotrons*. 1970.
- [4] D.A. Edwards; M. Syphers. *Longitudinal Motion*. Third. ISBN-10 981-02-3858-4, ISBN-13 978-981-02-3858-4. Alexander Wu Chao and Maury Tigner, 2009, pp. 67–68.
- [5] H. Wiedemann. *Particle Accelerator Physics*. Third. ISBN-13 978-3-540-49043-2. Springer, 2007, pp. 49–61.
- [6] H. Timko; T. Argyropoulos; T. Bohl; H. Damerau; J.F. Esteban Müller; S. Hancock; E. Shaposhnikova. *Experimental and Simulation Studies of the PS-to-SPS Beam Transfer Efficiency*. 2012.
- [7] H. Wiedemann. *Particle Accelerator Physics*. Third. ISBN-13 978-3-540-49043-2. Springer, 2007, p. 219.
- [8] P. Baudrenghien; T. Butterworth; F. Dubouchet; A. Pashnin; J. Noirjean; R. Olsen. *Rephasing SPS-LHC*. 2008.
- [9] D. Manglunki; M. Albert; M.E. Angoletta; G. Arduini; P. Baudrenghien; G. Bellodi; P. Belochitskii; E. Benedetto; T. Bohl; C. Carli; E. Carlier; M. Chanel; H. Damerau; S. Gilardoni; S. Hancock; D. Jacquet; J.M. Jowett; V. Kain; D. Küchler; M. Martini; S. Maury; E. Métral; L. Normann; G. Papotti; S. Pasinelli; M. Schokker; R. Scrivens; G. Tranquille; J.L. Vallet; B. Vandrope; U. Wehrle; J. Wenninger. "Ions for LHC: Towards Completion of the Injector Chain". In: CERN-AB-2008-058 (2008).
- [10] M.E. Angoletta; A. Blas; A. Butterworth; A. Findlay; F. Pedersen. "PSB LLRF Renovation: Initial Beam Tests of the New Digital Beam Control System". In: CERN-BE-Note-2009-021 (2009).
- [11] M. Benedikt; H. Damerau; S. Hancock. "A Straightforward Procedure to Achieve Energy Matching Between PSB and PS". In: AB-Note-2008-022(MD)Revised (2008).